

A method for applying matrix corrections to X-ray intensity maps using the Bence–Albee algorithm and Matlab

G. L. CLARKE,¹ N. R. DACZKO¹ AND C. NOCKOLDS²

¹*School of Geosciences F05, University of Sydney, Sydney, NSW 2006 Australia, (geoffc@mail.usyd.edu.au)*

²*Electron Microscope Unit F09, University of Sydney, Sydney, NSW 2006 Australia*

ABSTRACT Matlab scripts that apply the Bence & Albee (1968) matrix correction algorithm to X-ray intensity data collected as element maps on a Cameca SX-50 microprobe are used to produce two-dimensional maps of oxide weight percent and cation proportions for SiO₂, Al₂O₃, FeO, MnO, MgO, CaO, Na₂O and K₂O. Once generated, large data sets of mapped oxide weight percent values or cation numbers that retain spatial information can be used petrologically. The technique is used to evaluate the compositional range of barroisitic amphibole in an eclogite from New Caledonia, to examine aspects of equilibration during the partial hydration of the eclogite facies mineral assemblage.

Key words: equilibration; matrix correction; mineral zoning; X-ray map.

INTRODUCTION

Conventional microprobe analyses or profiles of analyses present a random or one-dimensional section that may miss critical zones or minerals present in small proportions. X-ray maps, generated using an electron microprobe, allow fine-scale two-dimensional spatial relationships between minerals to be shown, as well as characteristics of mineral zoning that may otherwise be difficult to detect. They are collected with the diffracting crystal in each wavelength dispersive spectrometer set to one wavelength to record X-ray intensity as the sample stage is stepped through a chosen area. The number of elements that can be counted simultaneously is dependent on the number of spectrometers. Image manipulation of these raw intensity X-ray maps has commonly needed expensive software and a Unix workstation, from which it has been difficult to export results. In addition, as element data in X-ray intensity maps are not proportional or corrected for partial X-ray re-absorption, they are not suitable for use in petrology. The new generation of fast personal computers offers the possibility of overcoming these limitations by the application of a comparatively simple algorithm for matrix correction to raw intensity maps. We outline a method to convert Visilog files collected using a Cameca SX-50 microprobe and Sun workstation into a format that can be manipulated on personal computers. The α -factor approach of Bence & Albee (1968) for matrix correction is applied to these data to produce two-dimensional maps of oxide weight percent and cation proportions for the eight major rock-forming elements. Data in the processed maps are much more petrologically informative than maps of X-ray intensity, as they can be queried using a variety of routine petrological methods. For example, the maps

can be used to calculate bulk rock compositions for domains that would not be possible using conventional chemical techniques. Alternatively, by applying appropriate thresholds, data relevant to any chosen mineral(s) can be isolated and presented as cation maps, maps of cation ratios or binary plots of cation proportions. It is a powerful technique for the study of rocks with chemically zoned minerals.

DATA COLLECTION

Data for this paper were collected using the Cameca SX-50 electron microprobe housed at the Electron Microscope Unit, University of New South Wales. Standard operating procedures involved a 15 kV accelerating voltage, 1–3 μ m beam size and a 20 nA beam current. The microprobe has four multicrystal wavelength-dispersive spectrometers and was operated with a configuration involving two TAP, one LIF and one PET diffracting crystals. Microprobe analyses reduced using the Cameca PAP matrix correction program (Pouchou & Pichoir, 1984) were used to test the Bence & Albee (1968) algorithm and our choice of α and β factors. The element maps were collected using Visilog software on a Sun workstation. The maps used in the examples below had nominal count times on each point of 300 ms. The count time was found to be systematically low, as there appears to be an unspecified dead time that is dependent on the distance between analysis points and the focal range required for the data collection; this is addressed further below. The distance between analyses in the element maps discussed below is 5 or 10 μ m.

The data presented below for each sample was collected in two mapping stages. The UNSW Cameca

SX-50 microprobe has four wavelength spectrometers, so data for the intensity of Na (TAP crystal), K (PET), Fe (LiF) and Al (TAP) were first mapped, and Mg (TAP), Ca (PET), Mn (LiF) and Si (TAP) were then collected as a second set of maps. Data collected from each spectrometer were converted to $n \times m$ intensity matrices using the method outlined below, and intensity data for each element combined into one $n \times m \times 8$ matrix. Routine petrological order is followed, with the Si data placed in the first layer, then Al, Fe, Mn, Mg, Ca, Na and K. All the scripts used below assume that this order is maintained.

CONVERTING VISILOG FILES

The Visilog files need to be copied to a computer with Matlab installed. The Matlab scripts below assume that the Image Processing Toolbox is installed, and that the Visilog files are in the same directory as the Matlab application. The Visilog files used below are stored in 16 bit binary files, with a 528 character header that contains information such as file size, wavelength and diffracting crystal. The Matlab script (Appendix 1) opens this file as a one-dimensional vector, removes the header information and then builds the appropriately-sized matrix for the element map. The new matrix is then presented graphically in Matlab using the *imagesc* (*matrix name*) command. If more than one element map is to be opened at any one time, the variable name *imagemtx* needs to be changed to avoid overwriting the older data matrix. Copies of the Matlab scripts used in this manuscript can be viewed at the URL <http://www.es.usyd.edu.au/geology/people/staff/Clarke/mappingWeb/mapkey.html>.

APPLYING THE BENCE-ALBEE METHOD OF MATRIX CORRECTION

The empirical approach of Bence & Albee (1968) involves two main assumptions (from Armstrong, 1984): (1) there is a simple hyperbolic relation between relative concentration, C , and relative X-ray intensity, K , in binary oxide systems, the curvature of which can be expressed in terms of α -factors such that $C/K = \alpha + (1 - \alpha) C$; and (2) that in ternary or more complicated oxide systems, the relation between relative intensity and relative concentration can be determined by a linear combination of α -factors such that:

$$\alpha = \frac{\sum_{i=1}^{i=n} c_i \alpha_i}{\sum_{i=1}^{i=n} c_i} \quad (1)$$

This matrix correction was applied to the maps of X-ray intensity, because it is simple and involves less computation than, for example, a ZAF or PAP correction. We used a matrix of α -factors calculated

by Love & Scott (1978; Appendix 2) using the ZAF correction procedure for an accelerating voltage of 15 kV and a take-off angle (being that between the specimen surface and the detected secondary X-rays) of 40° . Complex silicate minerals were mostly used as standards, requiring the calculation of β -factors for each element (Bence & Albee, 1968), using the α -factors from Love & Scott (1978) and the known concentration of oxides in the standards. Diopside was used as a standard for Ca, Mg and Si; sanidine was used as a standard for Al and K; rhodonite was used as a standard for Mn; chromite was used as a standard for Fe; and albite was used as a standard for Na. The β -factors calculated for the standards used with the UNSW microprobe are listed in Appendix 2.

The script used to apply the Bence & Albee (1968) algorithm is given in Appendix 2. To use this script on data collected elsewhere, the correct counts on the different standards need to be entered and new β -factors for these standards need to be calculated and entered (Bence & Albee, 1968). The method assumes a linear relationship between count time and X-ray intensity, and the script requests input of the count time used for each analysis point. Though the example maps were collected with a nominal count time of 300 ms, this nominal time includes machine dead time that is related to stage movement. Hence, the count time entered for the purpose of applying the Bence-Albee algorithm needs to be adjusted down to avoid low totals. Analyses of quartz were used to calibrate the true count time: from trial and error, 284 ms gave the best total for element maps collected at a nominal 300 ms and 10 μm point spacing.

The script given in Appendix 2 saves an $n \times m \times 8$ matrix containing weight percent oxide values. These can be converted to an $n \times m \times 8$ matrix containing cation proportions using the script given in Appendix 3. This script recalculates the weight percent data using 24 oxygen and assumes that all iron is ferrous. Apart from the advantages of having the elements in cation proportions, the recalculation circumvents difficulties outlined above with respect to the real count time.

DATA QUALITY

As an indication of data quality, we present cation maps and profiles of Si and Al cation values for part of a silica-poor granulite facies metapelite, taken from the Oygarden Group of Islands, Kemp Land, east Antarctica (Kelly *et al.*, 2000). Symplectites of sapphirine, orthopyroxene and plagioclase partially pseudomorph garnet. This sample is a good candidate with which to test the method, because it is mineralogically simple, and has large grains with limited chemical zoning. Figure 1 shows Si (a) and Al (b) cation values mapped over a portion of sample OG582 that contains a garnet grain and distinct secondary symplectites. The map was collected with a 5 μm spacing between analyses. Figure 2 shows profiles of Si (a) and Al (b)

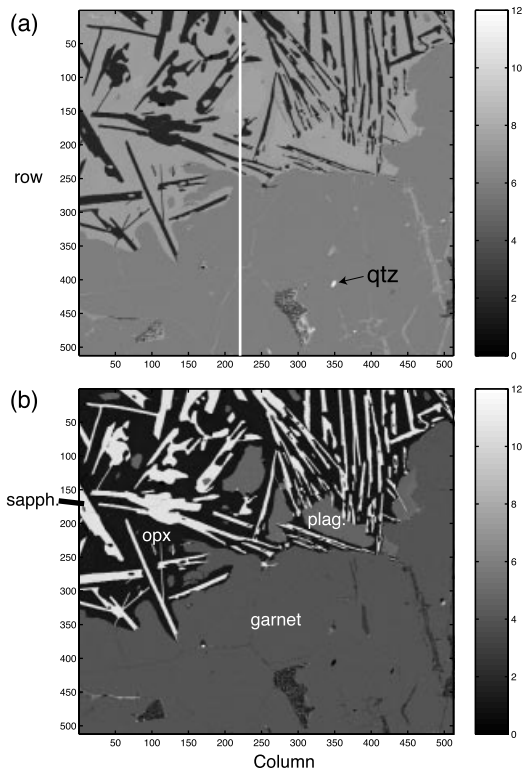


Fig. 1. Maps of Si (a) and Al (b) proportions for symplectites of sapphirine, orthopyroxene and plagioclase that partially pseudomorph garnet. X-ray intensity data were collected with a spacing of 5 μm , a count time of 300 ms, and recalculated for 24 oxygen. Sample OG582 from the Oygarden Group of Islands, Kemp Land, east Antarctica. Small proportions of quartz are preserved as inclusions in garnet. The line at column 220 is used to draw the profiles in Fig. 2.

cation values through column 220 on Fig. 1; garnet has been correctly recalculated to 6 Si cations and 4 Al cations (per 24 oxygen). Though not shown in the profiles, quartz (Fig. 1a) is correctly recalculated to 12 Si cations (per 24 oxygen). Each of the minerals is distinct in the maps due to their different Al and Si proportions.

As the data are collected with comparatively short count times (300 ms), care needs to be exercised in the analysis of elements present in low proportions or those with low X-ray intensities, for example Na, K and Fe. Table 1 presents the mean and standard deviation of the garnet analyses displayed in Fig. 1. Two populations of garnet data were extracted from the full element map, to test how sensitive the mean and standard deviation calculations were to the data filtering. We chose garnet analyses with more than 35% SiO_2 , and recalculated garnet analyses (per 24 oxygen) with more than 1.3 iron cations, and: (I) between 3.5 and 4.2 Al cations returning 115 272 analyses; or (II) between 3.5 and 4.5 Al cations returning 122 422 analyses. The two stages of data filtering, involving both weight percent and cation maps, avoids analyses with a low total

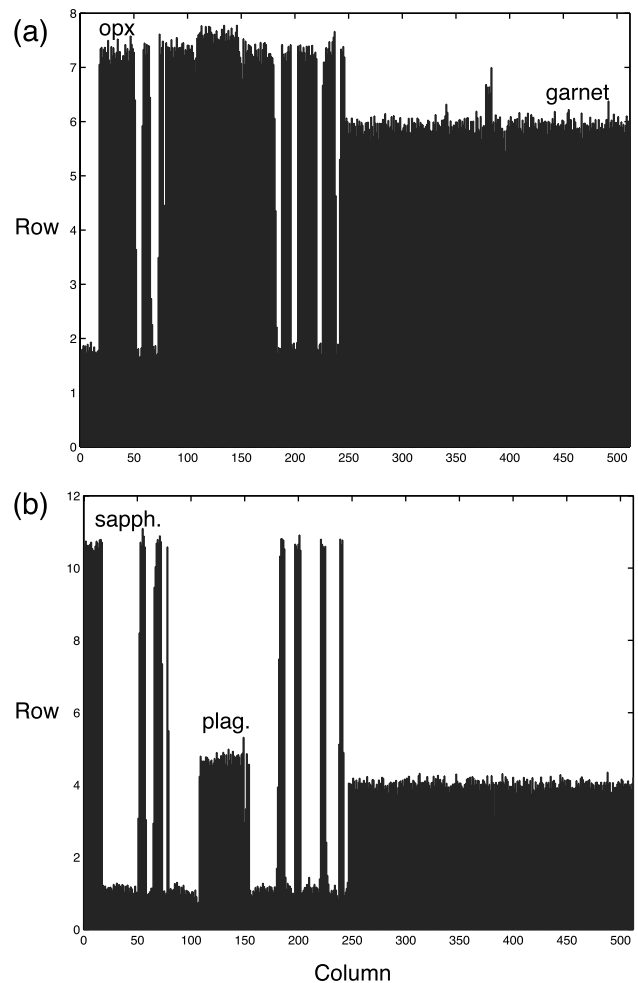


Fig. 2. Profiles of Si (a) and Al (b) cation values through column 220 in Fig. 1.

wt% being rescaled to apparently meaningful cation proportions.

The integrated analyses from a large proportion of a mineral grain, for data with a comparatively low standard deviation, will give a more representative result than isolated point analyses. Table 1 indicates a standard deviation of approximately 2% of silica and 2.5% of Al cation values in garnet analyses from sample OG582. Standard deviations for SiO_2 and Al_2O_3 values are slightly lower for the smaller population of garnet analyses, otherwise the two datasets have similar mean and standard deviation values (Table 1). SiO_2 and Al_2O_3 are the most reliable elements for plotting and performing image-analysis tasks such as data masking. Magnesium would be the next most reliable element in garnet in this sample, having a standard deviation close to 4.5% of the cation values. Iron is more problematic due to lower X-ray count values, and Mn and Ca give more uncertain results due to low concentration in this garnet grain. Higher proportions of grain edge

Table 1. Mean and standard deviation for weight percent and cation values of garnet analyses in sample OG582 (Figs 1 & 2). Garnet data were extracted from the full element map by generating binary maps in Matlab on the criteria of garnet analyses having more than 35% SiO₂, and the recalculated garnet analyses (per 24 oxygen) having more than 1.3 iron cations, and: (I) between 3.5 and 4.2 Al cations; or (II) between 3.5. and 4.5 Al cations. These two masks were then used to extract data from the maps of weight percent and cation values.

	From maps				Conventional analyses		
	3.5 < Al < 4.2 means	115272 analyses std dev	3.5 < Al < 4.5 means	122422 analyses std dev	grt1	grt2	grt3
SiO ₂	41.25	1.09	41.20	1.12	41.01	41.02	41.16
Al ₂ O ₃	23.66	0.89	23.74	0.93	23.50	23.34	23.41
FeO	13.6	1.31	13.57	1.31	14.98	16.04	14.96
MnO	0.54	0.29	0.54	0.29	0.41	0.461	0.41
MgO	19.25	1.00	19.21	1.04	18.02	17.23	17.93
CaO	1.68	0.27	1.68	0.27	1.82	1.976	1.74
Σ	100.16	2.75	100.11	2.77	99.733	100.07	99.61
num. ox.	24		24		24	24	24
Si	5.936	0.118	5.931	0.121	5.954	5.967	5.976
Al	4.014	0.103	4.027	0.115	4.022	4.003	4.008
Fe	1.635	0.143	1.632	0.144	1.819	1.951	1.817
Mn	0.066	0.035	0.066	0.035	0.051	0.057	0.050
Mg	4.126	0.176	4.120	0.184	3.900	3.735	3.879
Ca	0.259	0.042	0.259	0.042	0.283	0.308	0.270
Total	16.08	0.106	16.08	0.108	16.03	16.02	16.00

analyses will reduce the quality of data further for fine-grained mineral assemblages, or element maps collected using comparatively large steps between analyses. For example, analyses of the symplectites of Opx and sapphirine in Fig. 2 have approximately twice the proportional standard deviation for silica and cation values compared with those of garnet.

EXAMPLE: BARROISITIC ECLOGITE FROM NEW CALEDONIA

Metabasic eclogite facies assemblages that reflect conditions involving $P \approx 20$ kbar and $T \approx 600$ °C are preserved as cm to km-scale pods in hydrous glaucophanite in northern New Caledonia. The eclogite facies mineral assemblages mostly involve barroisitic amphibole, with less garnet, omphacite, phengite, rutile, clinozoisite and quartz (Clarke *et al.*, 1997). Garnet preserves comparatively simple bell-shaped zoning patterns of Mn content, which we infer to reflect growth during prograde metamorphism. Phengite, clinozoisite and omphacite that are intergrown with barroisite show a restricted compositional range in individual samples. Barroisite, which may form up to 70% of the eclogite assemblage, shows a comparatively large range in Si and Al content. This is inferred by Carson *et al.* (2000) to be related to the partial recrystallization of the eclogite facies assemblage during hydration and decompression of the terrane to conditions that involved $P \approx 12$ kbar and $T \approx 600$ °C.

The compositional variation shown by minerals in such rocks presents difficulties with respect to establishing which minerals and what compositions can be used for the purpose of thermobarometry, and what stage of a dynamic P - T path the compositions reflect. These problems can be overcome to some extent by the use of

pseudosections (e.g. Hensen, 1971; Powell *et al.*, 1998), which help in the textural interpretation of such complex rocks (Carson *et al.*, 2000). However, a critical step in drawing any pseudosection involves establishing an effective bulk rock composition (e.g. Stüwe, 1997). This is not a simple task in eclogites and blueschists. As many minerals are chemically zoned and may preserve distinct parts of the P - T history, an XRF analysis of the rock does *not* reflect an effective bulk rock composition for practically any stage in a rock's history. Element mapping has much to offer in the textural analysis of these rocks, especially when cation values can be mapped.

Sample 9341 is representative of the barroisitic eclogites in northern New Caledonia. A 512 × 512 map was collected at 10 μm steps, and the matrix-corrected data recalculated to 23 oxygen (Fig. 3a; Appendix 3) because most of the following discussion concerns amphibole composition. The chemistry of sodic-calcic amphibole can vary from actinolite through winchite to barroisite (Clarke *et al.*, 1997); for the case of simplicity, they will be referred to as hornblende. To examine hornblende compositional variations in detail, all other minerals may be excluded and a new matrix generated by selecting only data that have between 6.23 and 7.95 Si cations per formula unit (pfu), and more than 2.16 Mg cations pfu. These criteria were selected using the maps of cation values. The first criterion includes omphacite, which is eliminated by the second criterion, to generate a matrix with approximately 150 000 analyses of hornblende. Once generated, imaging of the hornblende map can be enhanced for the compositional variation shown by the hornblende grains, without the confusion provided by the chemical range of other minerals (Fig. 3b). Large hornblende grains can be distinguished with

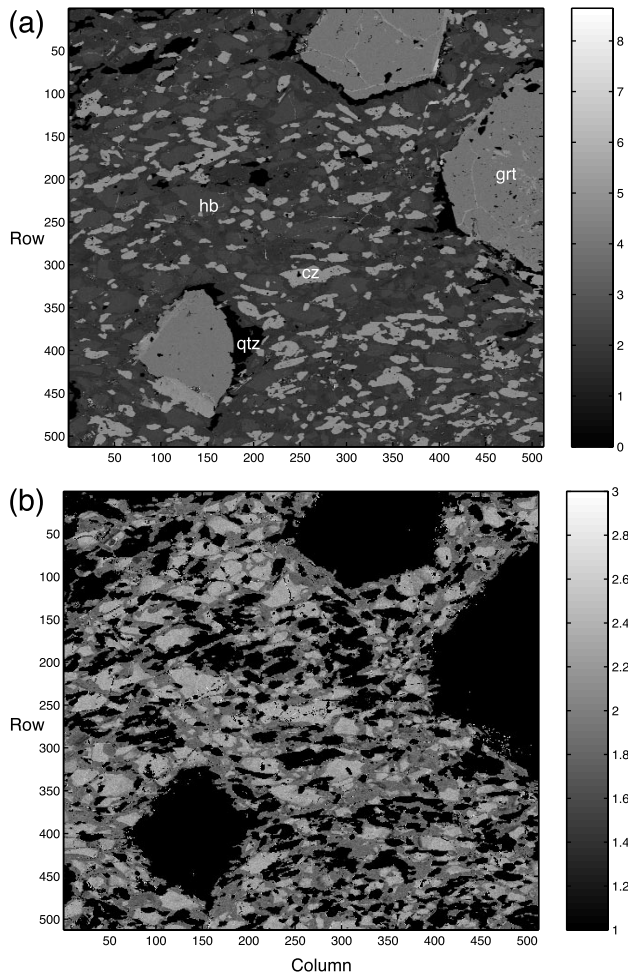


Fig. 3. (a) Map of Al cation values (23 oxygen) covering part of a barroisitic eclogite from the Pam Peninsula, northern New Caledonia. (b) Map of Al proportions in hornblende (23 oxygen), created by filtering out nonamphibole data in Fig. 3(a).

comparatively silica-poor, Al-rich cores and silica-rich, Al-poor rims. The core compositions of different grains are similar. To examine the variation in hornblende composition, the number of Si cations on each analysis is plotted against the number of Al cations (Fig. 4), with a two-dimensional negative correlation of -0.79 for the two data matrices. A plot of Ca cations vs. Si cations also indicates a strong negative correlation between these elements (2D correlation = -0.57). Such results can be used to infer exchange vectors controlling the variation in amphibole composition, but it is worthwhile noting that the data have several populations. Figure 5(a) is a plot of the Si cations per 23 oxygen vs. $X_{Na} = Na/(Na + Ca)$ for all amphibole data. The data show the two trends: (1) an overwhelming proportion of the data are barroisitic with variable Si content but consistent $X_{Na} \approx 0.5$; and

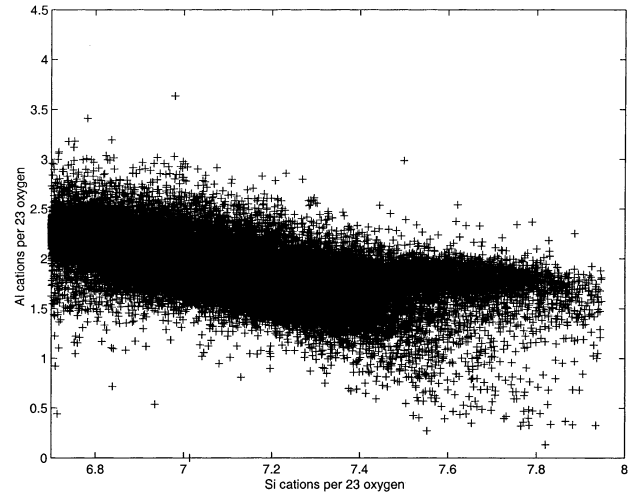


Fig. 4. Plot of Si cation value against Al cation value (23 oxygen) for all analyses of hornblende in the map used to create Fig. 3(b).

(2) a small population of the data are glaucophane with large X_{Na} values and large Si cation values. Glaucophane was not detected optically. As trends in the data are partially obscured by the large number of analyses, Fig. 5(b) is the same plot showing 2000 points randomly selected from the dataset.

A complex mix of hornblende and minor glaucophane occurs in sample 9341, both of which show a moderate compositional range. The composition of the hornblende that accompanied the development of other eclogite facies minerals can be addressed by filtering the amphibole data again, using an arbitrary cut-off of 1.92 Al cations per formula unit to separate core and rim data. Figure 6(a) shows a Si- X_{Na} plot for 500 randomly selected points with $Al > 1.92$; Fig. 6(b) is the same plot for 500 randomly selected points with in the dataset with $Al < 1.92$. Though the data cropping has not been perfect, Fig. 6(a) indicates that most hornblende cores have a comparatively restricted range of $Si = 6.7-7.2$ cations per 23 oxygen. The rim hornblende compositions have $Si = 7.1-7.4$ cations and a few analyses fall in the glaucophane field.

If at some time all hornblende had one composition, can we say anything with respect to the processes that formed the compositional zoning? The mean of each elemental matrix for each of the amphibole populations can be used to examine any spatial control on amphibole composition. In addition, the mean of submatrices can be used to examine any difference between amphibole near and far from what are commonly inferred to be influential minerals, such as garnet. For example, Stüwe (1997) presents a model for retrogressive recrystallization whereby large porphyroblasts, such as garnet, influence local effective equilibration volumes and retrograde minerals because garnet is commonly

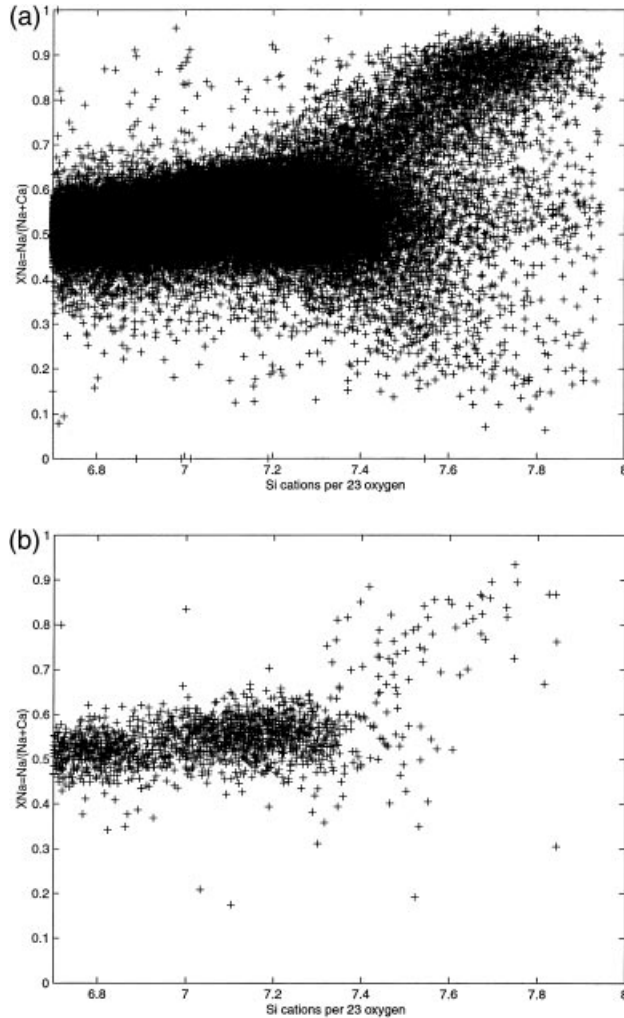


Fig. 5. (a) Plot of the Si cations (23 oxygen) vs. $X_{Na} = Na/(Na + Ca)$ for all analyses of hornblende in the map used to create Fig. 3(b). (b) Plot of the Si cations (23 oxygen) vs. X_{Na} for 500 hornblende analyses randomly selected from the data in Fig. 3(b).

the most ferrous mineral. During retrogression it could be expected to generate a localised, Fe-rich effective equilibration volume for some distance around the grain, compared with that for parts of the rock further away from the garnet porphyroblast. To test this hypothesis for the New Caledonian eclogite, the mean composition of hornblende in elemental submatrices near to garnet can be plotted against the mean composition of hornblende data distal to the garnet grains (Fig. 7a). A first order linear regression passes through all points, consistent with the two areas having identical elemental ratios. A slope for the regression different from 45° could reflect different hornblende compositions for the two areas. The data can be tested further by plotting the mean elemental ratios of the small matrix from near a garnet grain against the mean

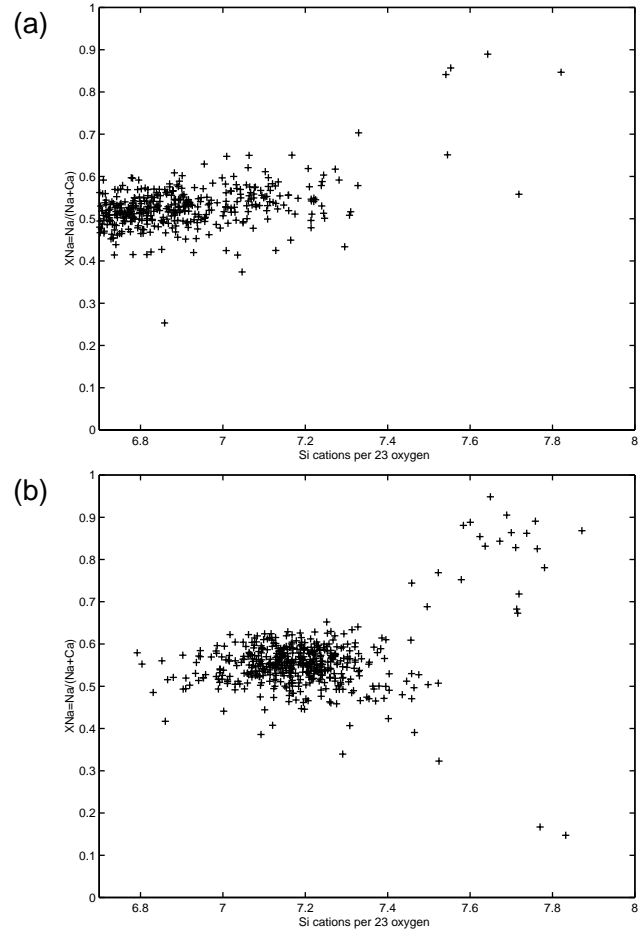


Fig. 6. (a) $Si-X_{Na} = Na/(Na + Ca)$ plot for 500 randomly selected analyses of hornblende cores, a subset of Fig. 3(b) with $Al > 1.92$. (b) $Si-X_{Na}$ plot for 500 randomly selected analyses of hornblende rims, a subset of Fig. 3(b) with $Al < 1.92$.

elemental ratio for the entire hornblende dataset (Fig. 7b). Again, a first order linear regression passes through all points, consistent with the interpretation that hornblende in this eclogite once had a restricted composition. On the basis of the discussion above, this composition was that now recorded by the cores of the hornblende grains. To examine changes induced by hornblende recrystallization subsequent to evolving $P-T$ conditions (Carson *et al.*, 2000), Fig. 7(c) presents a plot of the mean elemental ratios of the hornblende cores plotted against the mean elemental ratios of all hornblende. A first order linear regression passes through all points with the exception of Al, which lies less than 0.1 cation values away from the regression. The change in Al and Si contents of hornblende cores vs. rims (Fig. 3b) is reflected in this plot, though it is unclear which element(s) can be used as references to examine the change. Nonetheless, the plot is consistent with Si and Mn enrichment of the hornblende rims relative to their cores. Since the

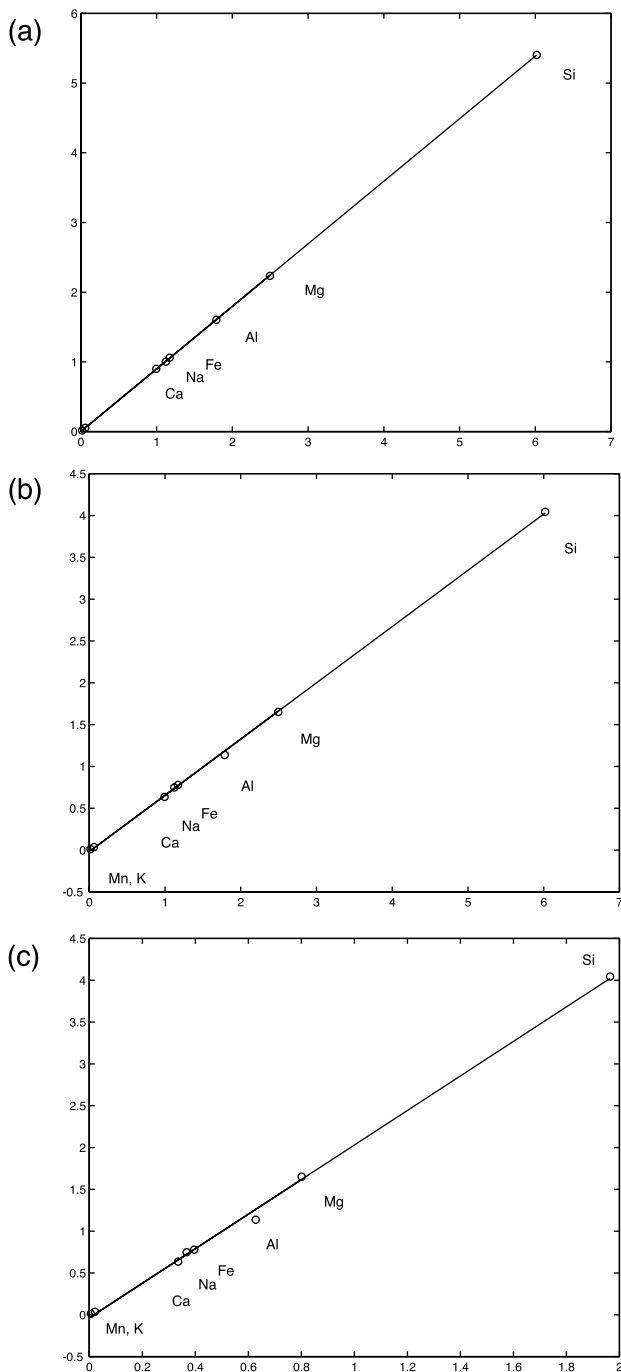


Fig. 7. (a) Mean composition of elemental submatrices of hornblende analyses made near to garnet (submatrix defined by rows 100–150 and columns 200–250 in Fig. 3b) plotted against the mean composition of hornblende analyses made distal to garnet grains (submatrix defined by rows 300–350 and columns 275–325 in Fig. 3b). Values on the axes are mean cation values for the respective domains. (b) Mean composition of elemental submatrices of hornblende analyses made near to garnet (submatrix defined by rows 100–150 and columns 200–250 in Fig. 3b) plotted against the mean composition of all hornblende analyses. (c) Mean composition of the hornblende cores plotted against all hornblende analyses.

compositions of hornblende cores of more than 200 μm width are comparatively uniform, the Si and Mn enrichment in the rims would have occurred due to limited cation exchange with adjacent minerals during retrogression. That the first order linear regressions in Fig. 7(a,b) pass through all points suggests that similar amounts of cation exchange occurred in all parts of the rock covered by the element map; i.e. proximity to garnet has not influenced the composition of retrograde hornblende.

CONCLUSIONS

The Bence & Albee (1968) matrix correction algorithm can be applied to maps of X-ray intensity data to produce two-dimensional maps of oxide wt% and cation proportions for the eight major rock-forming elements. Care needs to be exercised with the use of the data due to the comparatively low count times for each analysis, but the maps present a powerful method for the graphical representation of texturally complex rocks. Large volumes of individual mineral data can be extracted from the total map by applying appropriate compositional thresholds, and then plotted in a variety of petrologic methods. Bulk rock compositions can be generated for domains of texturally complex rocks, which would be otherwise impossible to obtain. The maps can be used to examine changes induced by the recrystallization of mineral grains during reaction or induced by evolving P – T conditions, in a manner that is more robust than that provided by random point analyses or one-dimensional profiles.

ACKNOWLEDGEMENTS

This work was supported by funding from an Australian Research Council Large Grant to GLC and R. Powell (A39905414). NRD was supported by an Australian Postgraduate Award. We thank B. Searle for extensive help with the UNSW electron microprobe, and N. Kelly for collecting the data used to draw Figs 1 and 2. Critical reviews by M. Williams and N. Pearson, and careful editorial work by R. Powell improved an earlier version of this paper.

REFERENCES

- Armstrong, J. T., 1984. Quantitative analysis of silicate and oxide minerals: a reevaluation of ZAF corrections and proposal for new Bence-Albee coefficients. In: *Microbeam Analysis* (eds Romig, A. D. & Goldstein, J. I.), pp. 208–212. San Francisco Press, San Francisco.
- Bence, A. E. & Albee, A. L., 1968. Empirical correction factors for the electron microanalysis of silicates and oxides. *Journal of Geology*, **76**, 382–403.
- Carson, C. J., Clarke, G. L. & Powell, R., 2000. Hydration of eclogite from the Pam Peninsula, New Caledonia. *Journal of Metamorphic Geology*, **18**, 79–90.

- Clarke, G. L., Aitchison, J. C. & Cluzel, D., 1997. Eclogites and blueschists of the Pam Peninsula, NE New Caledonia: a reappraisal. *Journal of Petrology*, **38**, 843–876.
- Hensen, B. J., 1971. Theoretical phase relations involving cordierite and garnet in the system MgO-FeO-Al₂O₃-SiO₂. *Contributions to Mineralogy and Petrology*, **33**, 191–214.
- Kelly, N. M., Clarke, G. L., Carson, C. J. & White, R. W., 2000. Thrusting in the lower crust: evidence from the Oygarden Islands, Kemp Land, east Antarctica. *Geological Magazine*, **137**, 219–234.
- Love, G. & Scott, V. D., 1978. Evaluation of a new correction procedure for quantitative electron probe micro analysis. *Journal of Physics*, **D-11**, 1369–1376.
- Pouchou, L. & Pichoir, F., 1984. A new model for quantitative X-ray microanalysis. *Recherche Aerospatiale*, **3**, 167–192.
- Powell, R., Holland, T. J. B. & Worley, B., 1998. Calculating phase diagrams with THERMOCALC: methods and examples. *Journal of Metamorphic Geology*, **16**, 577–588.
- Stüwe, K., 1997. Effective bulk composition changes due to cooling: a model predicting complexities in retrograde reaction textures. *Contributions to Mineralogy and Petrology*, **129**, 43–52.

Received 5 June 2000; revision accepted 23 April 2001.

APPENDIX 1: MATLAB SCRIPT TO CONVERT A VISOLOG FILE INTO A MATLAB MATRIX

```
% This script is to analyse element mapping (mxn) data from the probe
% and get it into a useable format
% Nathan Daczko 17.9.99
% Ask for the name of the file to be analysed.
thefile=input('Please give the filename of the file to be analysed in single quote marks. ');
numrows=input('Please give the number of rows in the image file matrix. Eg 256, 512 or 1024. ');
numcols=input('Please give the number of columns in the image file matrix. Eg 256, 512 or 1024. ');
% Open the .img file and get into a matrix (includes headers, etc.)
fid=fopen(thefile, 'r');
data1=fread(fid, 'int16');
status=fclose(fid);
% Chop off the standard known amount of characters (528)
% that belong to the file header.
headlength=528;
n=length(data1);
data2=data1((headlength+1):n);
INFO='Successfully chopped off header information
% Chop up data2 into numrows rows by numcols columns.
i=1;
temp=data2(i:(numcols),1);
temp=temp';
data3=temp;
i=i+numcols;
while i< length(data2),
temp=data2(i:(i+(numcols-1)),1);
temp=temp';
data3=[data3; temp];
i=i+numcols;
end
% Save the new matrix (imagemtx) for later use in Matlab or another program. (It
% will save time later if reloading data. i.e. no preprocessing involved.) The
% new file is named the first argument to the save command.
imagemtx=data3;
n=length(thefile);
savefile=thefile(:,1:n-4);
varname='imagemtx';
save(savefile,varname);
% Print image to screen to test result.
imagesc(imagemtx), axis image, colorbar;
```

APPENDIX 2: MATLAB SCRIPT TO PERFORM THE BENCE & ALBEE (1968) MATRIX CORRECTION ALGORITHM

```
% Bence-Albee matrix correction of X-ray maps
% Nathan Daczko 17-9-99
disp('');
disp(' *****');
disp(' Bence-Albee matrix correction procedure for X-ray maps');
disp('      Geoffrey Clarke and Nathan Daczko');
disp('      School of Geosciences');
disp('      Division of Geology and Geophysics');
disp('      University of Sydney');
disp(' *****');
disp('');
disp('');
```

```

% Ask for the name of the .mat file to be analysed.
thefile=input('Please give the filename of the .mat file to be analysed in single quote marks. ');
counttime=input('Please give the time (in seconds) that X-rays were counted for at each step. ');
iterate=input('Please give the number of times you wish the Bence-Albee to iterate (3 or greater. ');
% Open the .mat file into a variable called data
% Convert the data to a counts/ s format load(thefile);
data=eval(thefile);
data=data.*(1/counttime);
% Declare alpha-factors (Love & Scott alpha-factors (from Armstrong, 1984 Microbeam Analysis))
%
%      SiO2  Al2O3  FeO  MnO  MgO  CaO  Na2O  K2O
%
%      Si      1.000  1.494  1.279  1.211  1.431  1.048  1.356  0.987
%      Al      0.999  1.000  1.556  1.451  1.756  1.149  1.645  1.072
%      Fe      1.148  1.128  1.000  0.987  1.141  1.124  1.114  1.093
%      Mn      1.161  1.140  1.014  1.000  1.153  1.149  1.125  1.117
%      Mg      1.086  1.009  2.013  1.846  1.000  1.302  2.134  1.196
%      Ca      1.091  1.068  0.932  0.902  1.073  1.000  1.044  1.197
%      Na      1.352  1.242  3.066  2.778  1.130  1.741  1.000  1.564
%      K       1.144  1.118  0.987  0.959  1.120  0.858  1.088  1.000
alpha=[1.000  1.494  1.279  1.211  1.431  1.048  1.356  0.987
       0.999  1.000  1.556  1.451  1.756  1.149  1.645  1.072
       1.148  1.128  1.000  0.987  1.141  1.124  1.114  1.093
       1.161  1.140  1.014  1.000  1.153  1.149  1.125  1.117
       1.086  1.009  2.013  1.846  1.000  1.302  2.134  1.196
       1.091  1.068  0.932  0.902  1.073  1.000  1.044  1.197
       1.352  1.242  3.066  2.778  1.130  1.741  1.000  1.564
       1.144  1.118  0.987  0.959  1.120  0.858  1.088  1.000];
% Declare beta-factors for the standards
% beta values in vector in order: Si      Al      Fe      Mn      Mg      Ca      Na      K
beta=[1.0356423  1.3285742  1.0765097  1.0976045  1.2543714  1.0795094  1.3702150  1.0095439];
% Declare standards information (peak-background in counts/ s; concentration is wt% oxide)
%
%      Si      Al      Fe      Mn      Mg      Ca      Na      K
stdcounts=[9791.2  3727.2  559.2  993.2  2719.1  2579.5  1234.5  300.6];
stdconc=[0.5537  0.1876  0.1750  0.3766  0.1862  0.2537  0.1159  0.1211];
% Perform the matrix correction for each point in the matrix
[m,n,o]=size(data);
answer=zeros(m,n,o);
for h=1:m,
for i=1:n,
% Make the first approximation of the chemical composition of the unknown
% For each element k[E,U]=(I[E,U]/I[E,STD])*C[E,STD]/B[E,STD]
% where k[E,U] is wt% oxide for element E in unknown
% I[E,U] is intensity of counts of element E in unknown {get from element maps}
% I[E,STD] is intensity of counts of element E in standard {get from standards variable}
% C[E,STD] is wt% oxide concentration of element E in standard {get from conc. variable}
% B[E,STD] is beta-factor for element E in standard {get from beta variable}
concl=zeros(1,o);
for j=1:o,
concl(1,j)=(data(h,i,j)/stdcounts(1,j))*(stdconc(1,j)/beta(1,j));
end
conc2=concl;
for iteratenum=1:iterate,
% Make the first iteration
% The first approximation of the chemical composition is used to determine
% the correction factors (beta) using the relation:
% B[E,U]=(k[E1U]*a[E,E1]+k[E2U]*a[E,E2]+...k[En,U]*a[E,En])/(SUM(k(E1)...k(En)))
% where B[E,U] is beta correction-factor for element E in the unknown
% k[E1U]...k[En,U] are estimates of concentration made in the first approximation
% a[E,E1]...a[E,En] are the alpha-factors for element E1 ... n on element E
sumconc=sum(conc2);
beta1=zeros(1,o);
for j=1:o,
ka=0;
for k=1:o,
ka=ka+(conc2(1,k)*alpha(j,k));
end
beta1(1,j)=(1/sumconc)*ka;
end
% These new beta-factors are used to determine the next estimate of the chemical composition
% of the unknown: for each element the new k[E,U]=B[E,U]* old k[E,U]
conc2=zeros(1,o);
for j=1:o,

```

```

conc2(1,j)=(beta1(1,j))*(concl(1,j));
end
end
% Put the result into the answer matrix
answer(h,i)=reshape(conc2,1,1,o);
end
end
% Save the answer into a file called fnameba.mat where fname.mat was the input file
savefile=strcat(thefile, "ba");
assignin('base',savefile,answer);
save(savefile,savefile);

```

APPENDIX 3: MATLAB SCRIPT TO RECALCULATE MATRICES OF WEIGHT PERCENT INTO MATRICES OF CATION VALUES

```

% This script will recalculate microprobe data in an rxc8 array to give cation proportions
% for 24 oxygens (the number of oxygens can be changed using the variable NO below)
% Geoff Clarke 24-9-99
% It is set up to read r and c as locations with successively layered arrays
% of Si Al Fe Mn Mg Ca Na K
% It treats all Fe as Fe2
% Ask for the name of the .mat file to be analysed.
thefile=input('Please give the filename of the .mat file to be analysed in single quote marks. ');
load(thefile);
data=eval(thefile);
% declare MWO: the MW of oxides divided by the number of ox in order
% SiO2 Al2O3 FeO MnO MgO CaO Na2O K2O
% declare RMO: the ratio of metal to oxygen in each oxide
% declare NO: the number of oxygens for stoichiometry
MWO(1,1,1:8)=[30.045; 33.98; 71.85; 70.94; 40.32; 56.08; 61.98; 94.20];
RMO(1,1,1:8)=[0.5; 0.6667; 1; 1; 1; 1; 2; 2];
NO=24;
% loop through and recalculate each column of data, stepping through rows
[r,c,h]=size(data);
answer=zeros(r,c,h);
for i=1:r for j=1:c
% perform the first calculation of oxide wt percentage divided by MWO
% and calculate F=NO/sum(calc1)
calc1=data(i,j)./MWO;
F=NO/sum(calc1);
% then calculate the cation number by multiplying F by calc1 by RMO
answer(i,j)=F*(calc1.*RMO);
end end
% Save the answer into a file called fnamep.mat where fname.mat was the input file
savefile=strcat(thefile, "p");
assignin('base',savefile,answer);
save(savefile,savefile);

```